Journal of Engineering and Development, Vol. 15, No. 1, March (2011) ISSN 1813-7822

Shear Behavior Of RC Beams Strengthened With Varying Types Of FRP Materials Using Finite Element Analysis

Hanadi Fadhel Naji
lecturer
Civil Engineering Dept.
College of Engineering
Al-Mustansiriya University

Shaymaa Khalid Abdulrahman
Assistant lecturer
Civil Engineering Dept.
College of Engineering
Al-Mustansiriya University

Hiba Emad Abass
Assistant lecturer
Civil Engineering Dept.
College of Engineering
Al-Nahrain University

Abstract

The purpose of this study is to present a model suitable for analyzing RC beams strengthened with various types of FRP materials failing in shear using the finite element method. The finite elements adopted by ANSYS (Release-12, 2009) computer program were used in this study. The numerical analysis incorporates material nonlinearity due to concrete cracking in tension, nonlinear stress-strain relations of concrete in compression, crushing of concrete and yielding of steel reinforcement. Also the evaluation of the enhancement in shear strength of RC beams strengthened with FRP materials is investigated. Different types of RC beams strengthened with various types of FRP materials (carbon fiber reinforced polymer (CFRP), carbon fiber sheet (CFS), and glass fiber reinforced polymer (GFRP)) have been analyzed, and the finite element solutions are compared with the available experimental data. The finite element results obtained were the load-deflection response, stress distribution in concrete, stresses distribution in FRP materials and crack patterns. Several parametric studies have been carried out to investigate the effects of some important numerical and material parameters on the behavior of strengthened RC beams.

These parameters are effects of partial and full interaction between FRP materials and concrete surface, distribution of FRP materials stresses, and crack pattern. In general, good agreement between the finite element solutions and the available experimental results has been obtained. It was found that by assuming partial interaction between the FRP materials and concrete surface using interface elements, the ultimate load is decreased by about 4.2% to 6.17% for RC beam strengthened with FRP strips and 1.16% to 3.2% for RC beam strengthened with FRP sheets as compared with full interaction case. The RC beams strengthened with FRP sheets sustained cracks more than the RC beam strengthened with FRP strips and the RC beam strengthened with FRP strips sustained cracks more than the RC beam without strengthened.

الخلاصة

الهدف من هذه البحث هو تقديم إنموذج مناسب لتحليل العتبات الخرسانية المسلحة المقواة بالأنواع المختلفة من ألياف الفايبر البوليمرية (التي تفشل بالقص) باستخدام طريقة العناصر المحددة. تم اعتماد البرنامج الحاسوبي ANSYS (الإصدار الثاني عشر, 2009) لتحليل الإنموذج المقدم في هذه الدراسة. هذا الأسلوب يعتبر أن المواد لا تتصرف تصرفا خطيا تبعاً إلى تشقق الخرسانة والتصرف اللاخطي للخرسانة تحت الضغط وتهشم الخرسانة وخضوع حديد التسليح. أيضا تهدف الدراسة إلى إيجاد الزيادة الحاصلة في سعة القص للعتبات الخرسانية الناتجة عن استخدام الأنواع المختلفة من ألياف الفايبر البوليميرية. تم تحليل أنواع مختلفة من العتبات الخرسانية المقواة بأنواع ألياف الفايبر البوليمرية (ألياف الكربون البوليمرية (CFRP) و صفائح ألياف الكربون (CFS) و ألياف الزجاج البوليميرية (GFRP)) وقورنت النتائج المستحصلة لمنحنيات الحمل – الإزاحة (Load-Deflection) بطريقة العناصر المحددة مع النتائج المختبرية المتوفرة. تم التعبير عن النتائج عن طريق منحنيات الحمل – الإزاحة وتوزيع الاجهادات في الخرسانة وأيضا توزيع الاجهادات في ألياف الفايبر البوليمرية.

أجريت دراسة لتحري تأثير بعض المتغيرات المهمة على سلوك العتبات الخرسانية المقواة بأنواع مختلفة من ألياف الفايبر البوليمرية, تضمنت هذه الدراسة تأثير الترابط الجزئي و التام بين الألياف وسطح الخرسانة وتوزيع إجهادات الشد في شرائح الألياف. بشكل عام تم الحصول على توافق جيد بين النتائج التحليلية بطرقة العناصر المحددة والنتائج المختبرية. و تم أيضا دراسة توزيع التشققات في الخرسانة على طول فضاء العتبة. كذلك عند فرض ترابط جزئي بين الألياف وسطح الخرسانة يقل الحمل الأقصى بمقدار يتراوح بين 4,2% و 6,17% للعتبات الخرسانية المقواة بشرائح ألياف الفايبر البوليميرية ويقل بمقدار يتراوح بين 1,16% و 3,2% للعتبات الخرسانية المقواة بصفائح ألياف الفايبر البوليمرية بالمقارنة مع حالة التحليل باستخدام ترابط تام. العتبات الخرسانية المقواة بصفائح ألياف الكربون البوليمرية تتحمل تشققات أكثر من العتبات الخرسانية المقواة بشرائح ألياف الكربون البوليمرية و أن العتبات الخرسانية المقواة بشرائح ألياف الكربون البوليمرية تتحمل تشققات أكثر من العتبات غير المقواة.

1. Introduction

Fiber Reinforced Polymer (FRP) materials have been found to be successful for flexural strengthening, shear strengthening and ductility enhancement of concrete structures. Strengthening reinforced concrete (RC) beams with FRP composites is becoming an attractive alternative for the construction industry. These laminates offer all the advantages of composite materials, such as immunity to corrosion, a low density, and a high strength to weight ratio. [1]

Externally bonded steel plates, steel or concrete jackets and external post-tensioning are just some of the many traditional techniques available. Composite materials made of fibers in a polymeric resin, also known as Fiber Reinforced Polymers (FRP), have emerged as an alternative to traditional materials and techniques. The FRP system is defined as all the fibers and resins used to create a composite laminate, all applicable resins used to bond it to the concrete substrate, and all applied coatings used to protect the constituent materials. [2]

This system provides advantages over the traditional technique: lightweight, relatively easy installation and non-corrosivenes1-4. Most common FRP materials among a variety of kinds may include carbon fiber reinforced polymer (CFRP), carbon fiber sheet (CFS), and glass fiber reinforced polymer (GFRP). The products of these materials may be available in various forms with different fiber volume, resin matrix, fiber orientation, and dimension.

The main objective of this work is to investigate the overall shear behavior of RC beams strengthened with various types of FRP materials using finite element technique. The nonlinear material parameters considered in the nonlinear analysis are; cracking and crushing of concrete, inelastic response of concrete in compression and yielding of reinforcing steel.

2. Finite Element Model

2.1 Concrete Brick Element

Concrete is represented by the SOLID65 isoparametric brick element shown in Figure 1. This element has eight nodes with three degrees of freedom at each node (translations u, v, and w in the nodal x, y and z directions respectively) [3].

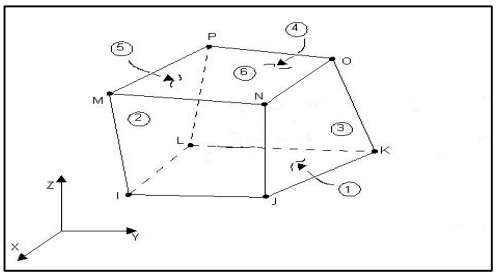

Figure 1 Brick element with 8-nodes SOLID65 [3].

2.2 Reinforcement Representation

LINK8 which has been used to model the reinforcement is a bar (or truss) element which may be used in a variety of engineering applications. This 3-D spar element is a uniaxial tension-compression element with three degrees of freedom at each node. Translation in the nodal x, y, and z directions. As in a pin-jointed structure, no bending of the element is considered. This element is used in the present study to simulate the behavior of reinforcing bars which works as stirrups in resisting the vertical shear in concrete and main steel reinforcement in resisting the flexural stresses. The geometry, node locations, and the coordinate system for the element are shown in Figure 2 [3].

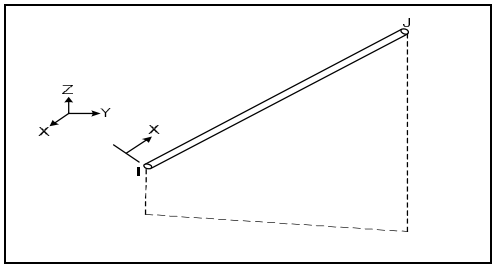

Figure 2 LINK8 3-D spar [3].

2.3 FRPs Reinforcement Representation

The 4-node quadratic-order membrane shell element (SHELL41) shown in Figure 3 is used in the present work to model the FRP. This element has four corner nodes with three degrees of freedom u, v, and w in the x, y, and z direction respectively at each node [3].

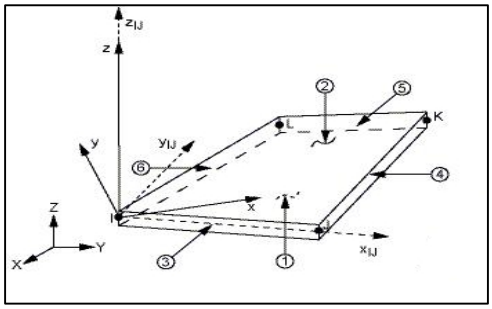

Figure 3 SHELL41 element [3].

2.4 Interface Element Representation

The 5-node pyramid contact element (CONTAC49) shown in Figure 4 is used in the present work to model the slip at interface between FRP and concrete surface. Each node in this element has three degrees of freedom u, v, and w in the x, y, and z directions respectively at each node [3].

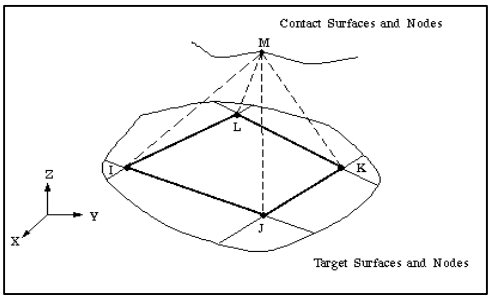

Figure 4 CONTAC49 element [3].

2.5 Numerical Integration

In the present work, the Gauss quadrature method will be used, since it has proved useful in finite element work [4]. The element stiffness matrix for brick element may be written in the form:

$$I = \int_{-1}^{1}\int_{-1}^{1}\int_{-1}^{1} F(\xi,\eta,\zeta)\,d\xi\,d\eta\,d\zeta$$

The integration rule used in this work is the 8 (2×2×2) points rule.

The solution of the set of equilibrium equations is based upon obtaining a balance between the external and internal load vectors such that the residual forces are zero. The basic nonlinear solution techniques, which have been used in connection with the finite element analysis, are the incremental technique, iterative technique and a combination of them (incremental-iterative technique). The incremental-iterative technique is widely used especially in the nonlinear analysis of RC structures. The load is applied incrementally and at each increment of loading successive iterations is performed, in order to obtain a converged solution [5]. This method yields a higher accuracy but with a large cost of computational effort. ANSYS-12[3] employs the "Newton-Raphson" approach to solve nonlinear problems. In this approach, the load is subdivided into a series of load increments. The load increments can be applied over several load steps. Figure 5 illustrates the use of Newton-Raphson equilibrium iterations in a single DOF nonlinear analysis.

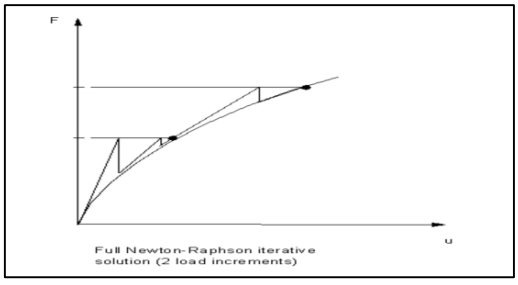

Figure 5Newton-Raphson equilibrium iterations in a single DOF [3].

In the nonlinear finite element analysis, convergence is assumed to occur when the difference between the external and internal forces has reached an acceptable small value. The force convergence criterion, which has been adopted in the current study, is based on out of balance forces and can be written in the form:

$$\frac{\|\{r\}\|}{\|\{f\}\|} \times 100\,\% \leq \text{TOLER}$$

where,

$$\|\{r\}\| = \left(\{r\}^T \{r\}\right)^{1/2}$$

$$\|\{f\}\| = \left(\{f\}^T \{f\}\right)^{1/2}$$

and TOLER is a specified convergence tolerance [6]. In this present study a value of 0.05 is specified for the convergence tolerance.

3. Outline of the Computer Program

The present study uses the computer program **ANSYS** version 12(**AN**alysis **SYS**tem) for performing the nonlinear model analysis. ANSYS is comprehensive general purpose finite element computer program that contains over 100,000 lines of code and more than 180 different elements. The program contains many special features which allow nonlinearities or secondary effects to be included in the solution. In this study, analyses of RC beams strengthened with various types of FRP materials failing in shear have been carried out and achieved using this computer program.

4. Modeling of Material Properties

4.1 Modeling of Concrete

4.1.1 Modeling of Concrete in Compression

The behavior of concrete in compression can be simulated in ANSYS-12 by an elasto-plastic work hardening model followed by a perfectly plastic response, which is terminated at the onset of crushing. The model used for compression is expressed in terms of yield criterion which is adopted in ANSYS-12 by the von-Misses criterion [3], a hardening rule which is adopted by ANSYS-12 assumes that the yield surface expands uniformly without distortion as plastic deformation occurs and a flow rule.

4.1.2 Behavior of Concrete in Tension

Linear elastic model prior to cracking is usually used to simulate the behavior of concrete in tension. In general, the cracking criterion of concrete is expressed in terms of principal tensile stresses or strains.

In the ANSYS-12, the onset of cracking is controlled by a maximum principal stress criterion. A smeared crack model with fixed orthogonal cracks is adopted to represent the fractured concrete.

4.1.3 Cracking Criterion

Three different approaches for crack modeling have been employed in the analytical studies of concrete structures using the numerical technique of the finite element method. These are smeared cracking modeling as shown in Figure 6, discrete cracking modeling as shown in Figure 7, and fracture mechanics modeling. For (ANSYS-12) computer program [3], crack modeling of concrete depends on smeared cracks.

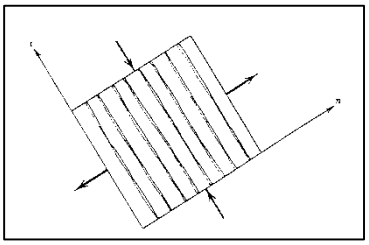

Figure 6 Representation of a single crack in the smeared crack modeling approach [7].

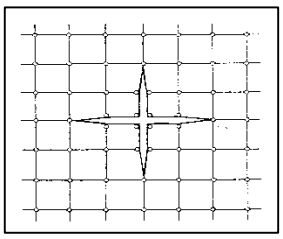

Figure 7 Two dimensional cracking representations in discrete crack modeling approach [7].

4.1.4 Crushing Modeling

If the material at an integration point fails in uniaxial, biaxial or triaxial compression, the material is assumed to crush at that point. Under this condition, the material strength at the considered integration point is assumed to have degraded to an extent such that its contribution to the stiffness of an element in question can be ignored (ANSYS-12) [3].

4.1.5 Failure Criterion for Concrete

The model to be used is capable of predicting failure for concrete materials. Both cracking and crushing types of failure model are accounted for. The two input strength parameters (i.e. ultimate uniaxial tensile and compressive strengths) are needed to define a failure surface of concrete. Consequently, a criterion for failure of concrete due to multiaxial stress states can be calculated [8].

The limiting tensile stress required to define the onset of cracking can be calculated for states of triaxial tensile stress and for combinations of tension and compression principal stresses. The stress function adopted in the present work has been used by William and Warnke [3]. Both the function of stress and the failure surface are expressed in terms of principal stresses denoted as σ_1, σ_2 and σ_3

where, $\sigma_1 = \max(\sigma_x, \sigma_y, \sigma_z)$

$$\sigma_3 = \min(\sigma_x, \sigma_y, \sigma_z)$$

and if $\sigma_1 \geq \sigma_2 \geq \sigma_3$, the failure of concrete is categorized into four domains:

1. $0 \geq \sigma_1 \geq \sigma_2 \geq \sigma_3$ (compression- compression- compression).
2. $\sigma_1 \geq 0 \geq \sigma_2 \geq \sigma_3$ (tension- compression- compression).
3. $\sigma_1 \geq \sigma_2 \geq 0 \geq \sigma_3$ (tension- tension- compression).
4. $\sigma_1 \geq \sigma_2 \geq \sigma_3 \geq 0$ (tension- tension- tension).

4.2 Modeling of Reinforcement

Modeling of reinforcement in connecting with the finite element analysis of RC members is much simpler than modeling of concrete. The uniaxial stress-strain relation for reinforcement is idealized in ANSYS-12 as a bilinear curve, representing elasto-plastic behavior with strain hardening. The relation is assumed to be identical in tension and in compression as shown in Figure 8.

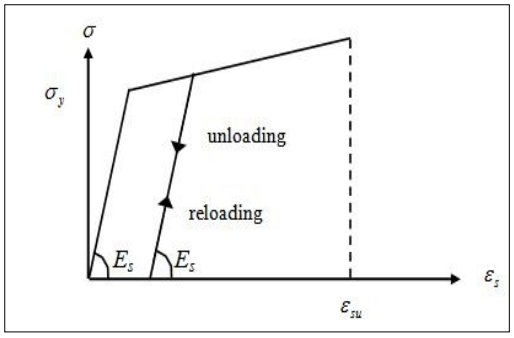

Figure 8 Stress-strain relationship of reinforcing bars [7].

4.3 Modeling of Fibers Reinforced Polymers (FRPs)

The behavior of fibers reinforced polymers (FRPs) used in the present study is assumed to have linearly elastic stress-strain relationship up to failure and does not exhibit any plastic deformation before rupture as shown in Figure 9.

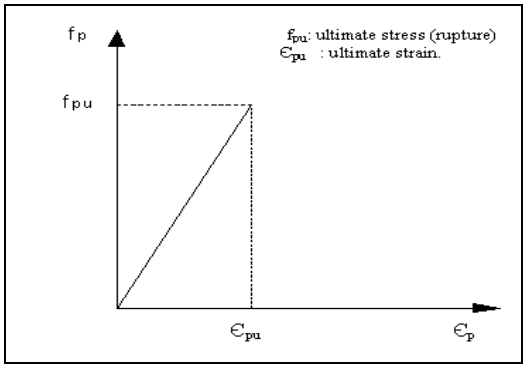

Figure 9 Idealization stress-strain relationships for FRP materials [9].

Failure of fiber reinforced polymers FRPs occurs when the strain (ε_{pu}) corresponding to the rupture stress (f_{pu}) is reached.

5. Model Verification

The aim of this study is to verify the adopted nonlinear finite element model by investigating the shear behavior of RC beams strengthened with various types of FRP materials. These examples were analyzed using ANSYS-12, while these examples were resolved using ANSYS-5.4 since the interface elements which were used to solve the problem are not found in version 12.

5.1 RC Beams Strengthened with Various Types of FRPs

These RC beams, which have been tested by Sim and et al. [10] were reinforced with various types of FRP materials instead of the stirrup reinforcement. Beams were simply supported over a 1600 mm span and were 250 mm wide and 250 mm deep.

The beams were reinforced with longitudinal steel bars and strengthened with external FRPs strips/sheets. They were subjected to two-point loads. Loading arrangement and reinforcement details together with the overall geometry of the beam are shown in Figures (10 to 12).

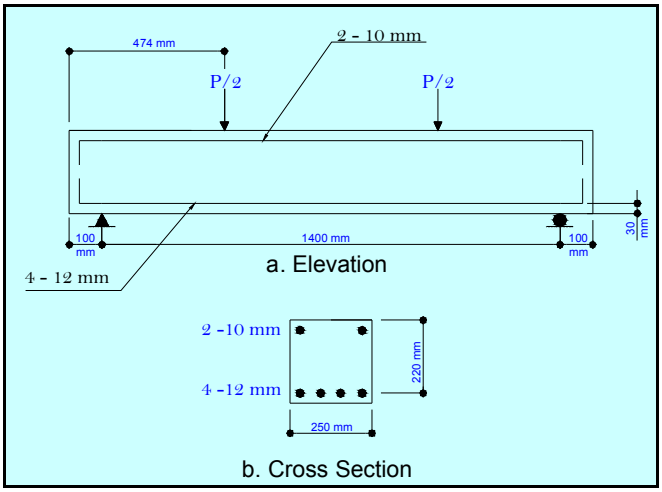

Figure 10 Dimension and loading arrangement of RC control beam.

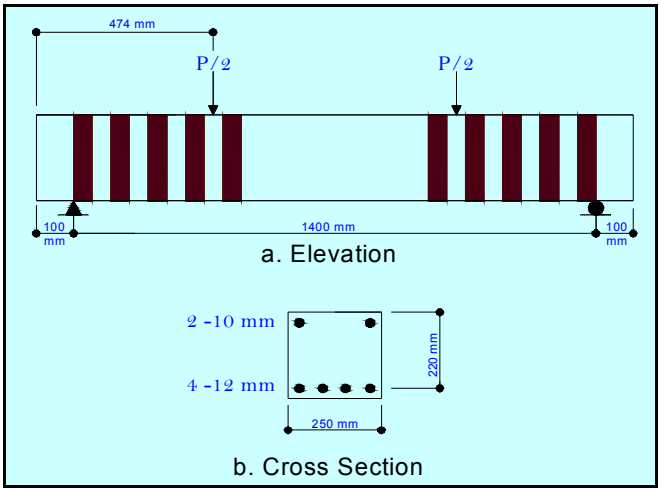

Figure 11 Dimension and loading arrangement of RC stripping beam.

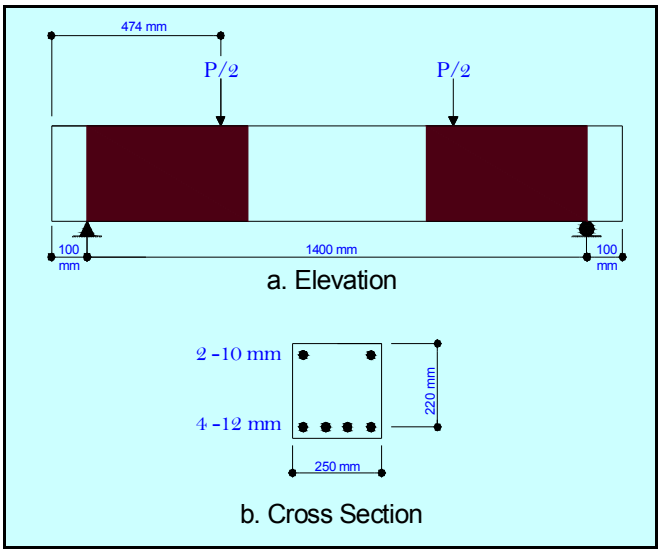

Figure 12 Dimension and loading arrangement of RC U wrapping beam.

The examples analyzed by ANSYS-12 are:

1. RC control beam (CON).
2. RC beam (CP90II) strengthened with U-wrapped CFRP sheets.
3. RC beam (CP90S) strengthened with CFRP strips.
4. RC beam (CS90II) strengthened with U-wrapped CFS sheets.
5. RC beam (CS90U) strengthened with CFS sheets.
6. RC beam (GS90II) strengthened with U-wrapped GFRP sheets.
7. RC beam (GS90S) strengthened with GFRP strips.

5.1.1 Finite Element Idealization and Material Properties

By taking into consideration the advantage of geometric and loading symmetry, one-quarter of the beams were taken for the analyses. The chosen segment was modeled using SOLID65 brick elements (8-node) for concrete. The main reinforcement was modeled using discrete representation by using LINK8 (2-node) elements, while the FRP materials were modeled using the SHELL41 (4-node) elements. The Beams are strengthened with various types of FRP materials. The concentrated loads were modeled as line loads uniformly distributed across the width of the top surface. The finite element analysis was carried out using 8-point integration rule, with a convergence tolerance of 5%. The shear transfer coefficients for an open crack β_0=0.2 and the shear transfer coefficients for a closed crack β_1=0.7. The full Newton-Raphson method has been adopted as nonlinear solution algorithm. The finite element mesh, boundary and symmetry conditions and loading arrangement used are shown in Figures (13 to 15). Material properties and the additional material parameters adopted in the analysis are shown in Table1.

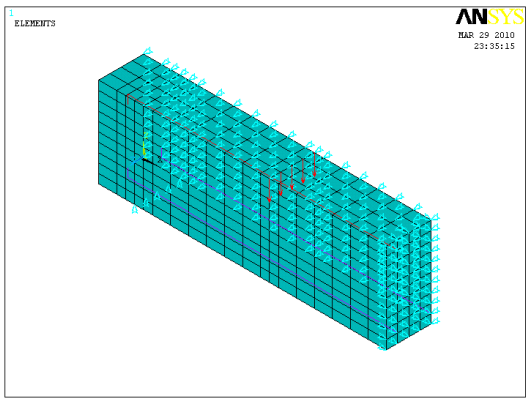

Figure 13 Finite element mesh, boundary and symmetry conditions used for RC beam (CON).

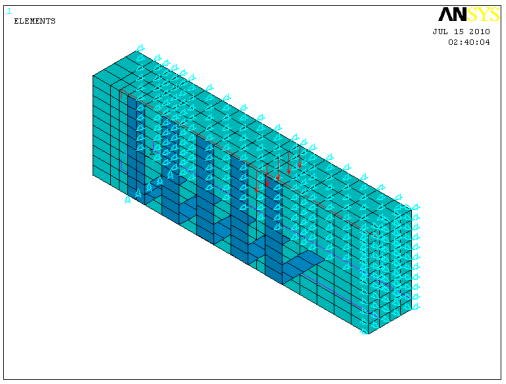

Figure 14 Finite element mesh, boundary and symmetry conditions used for RC beam (CP90S).

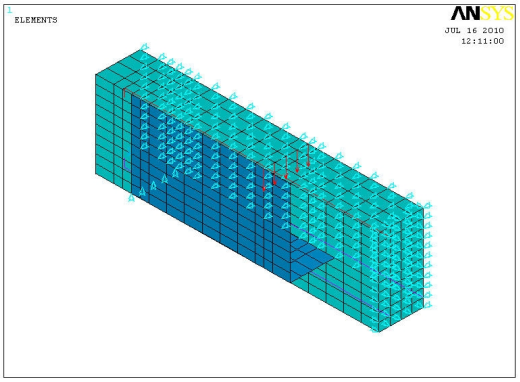

Figure 15 Finite element mesh, boundary and symmetry conditions used for RC beam (CP90II).

Table 1 Material properties and material parameters used for RC beams strengthened with FRP.

Concrete		
E_c	Young's modulus (MPa)*	23025
f_c`	Compressive strength (MPa)	24
f_t	Tensile strength (MPa)	2.4
v_c	Poisson's ratio**	0.15
Longitudinal reinforcement		
E_s	Young's modulus (MPa)**	200000
f_y	Yield stress (MPa)	400
v_s	Poisson's ratio**	0.3
A_s	Area of single longitudinal bottom bars (mm^2)	133
A_s	Area of single longitudinal top bars (mm^2)	79
CFRP		
t	Thickness (mm)	0.12
E_f	Young's modulus (MPa)	160000
v_f	Poisson's ratio[11]	0.3
f_y	Ultimate tensile strength (MPa)	3160
GFRP		
t	Thickness (mm)	0.12
E_f	Young's modulus (MPa)	23000
v_f	Poisson's ratio[11]	0.3
f_y	Ultimate tensile strength (MPa)	450
CFS		
t	Thickness (mm)	0.12
E_f	Young's modulus (MPa)	24000
v_f	Poisson's ratio[11]	0.3
f_y	Ultimate tensile strength (MPa)	3500

* $E_c = 4700\sqrt{f_c'}$ [12], ** Assumed value

5.1.2 Results of Analysis of RC beams strengthened with FRP materials

The experimental and analytical load-deflection curves obtained for RC control beam and RC beams strengthened with FRP materials are shown in Figures (16 to 23). The finite element solution is in acceptable agreement with the experimental results throughout the entire range of loading.

A relatively stiffer numerical curve is obtained at post-cracking stages of behavior. The numerical ultimate load was slightly lower than the experimental value. The numerical ultimate loads and the experimental ultimate loads are shown in Table 2.

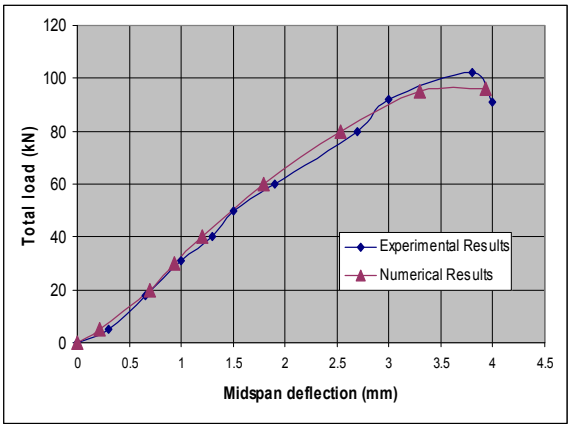

Figure 16 Experimental and numerical load-deflection behavior of RC control beam (CON).

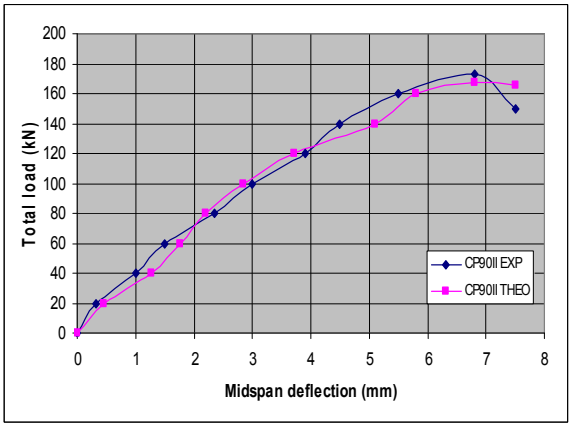

Figure 17 Experimental and numerical load-deflection behavior of RC beam (CP90II).

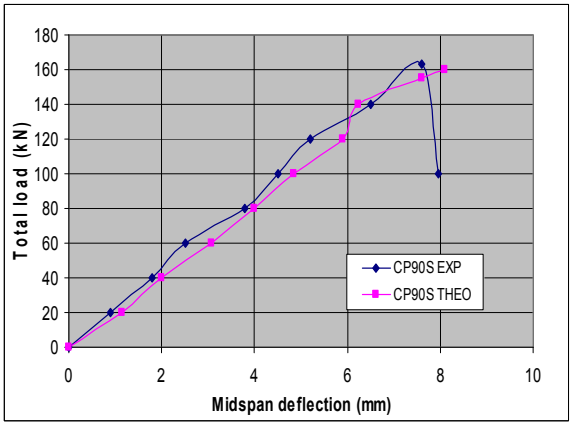

Figure 18 Experimental and numerical load-deflection behavior of RC beam (CP90S).

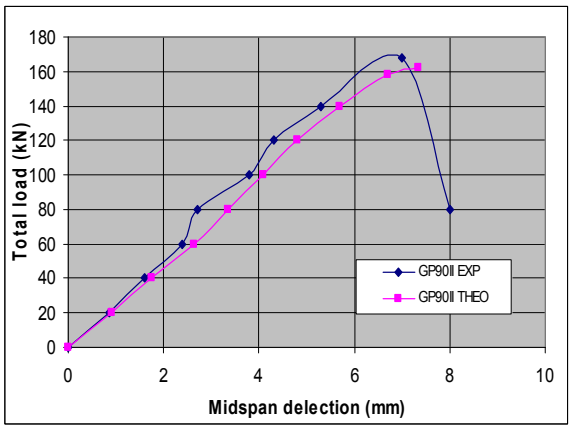

Figure 19 Experimental and numerical load-deflection behavior of RC beam (GP90II).

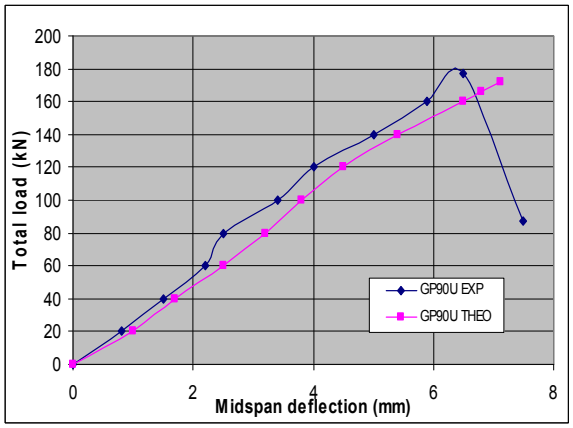

Figure 20 Experimental and numerical load-deflection behavior of RC beam (GP90U).

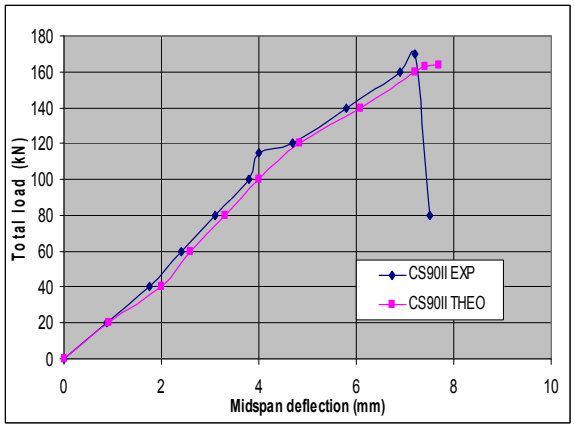

Figure 21 Experimental and numerical load-deflection behavior of RC beam (CS90II).

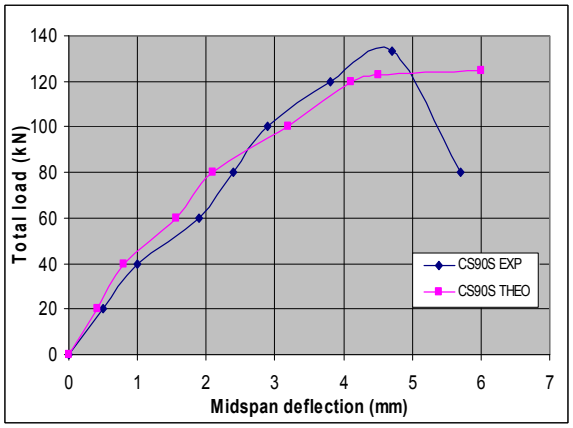

Figure 22 Experimental and numerical load-deflection behavior of RC beam (CS90S).

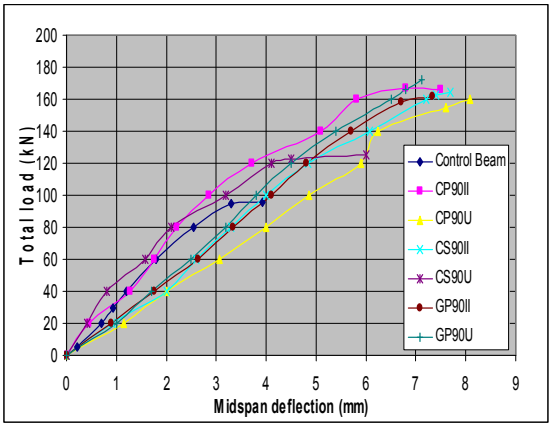

Figure 23 Numerical load-deflection behavior of RC beams strengthened with FRP materials.

Table 2 numerical ultimate loads and the experimental ultimate loads for RC control beam and RC beams strengthened with FRP materials.

Designated of the beam	Ultimate experimental load (kN)	Ultimate Finite Element load (kN)	Experimental load / F.E. load
CON	105	96	1.093
CP90II	173	166	1.042
CP90S	163	160	1.018
CS90II	170	164	1.036
CS90S	133	125	1.064
GS90II	168	162	1.037
GS90U	177	172	1.029

Variation of concrete stresses at the ultimate load level in the longitudinal x-direction (SX) along the selected quarter of control beam (CON) is shown in Figure 24.

Variation of CFRP stresses in y-direction (SY) at ultimate load level along the selected quarter of beam (CP90U) is shown in Figure 25.

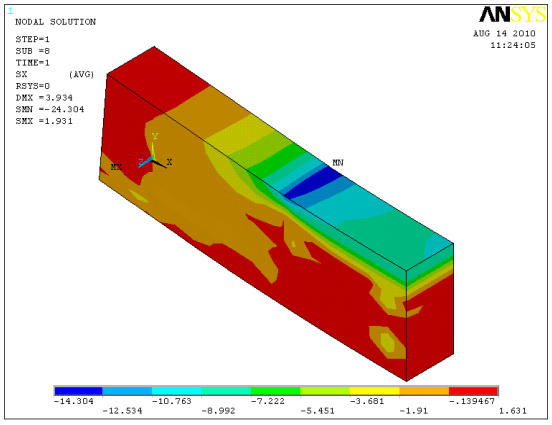

Figure 24 Variation of concrete stresses in x-direction along the selected quarter of RC control beam (CON).

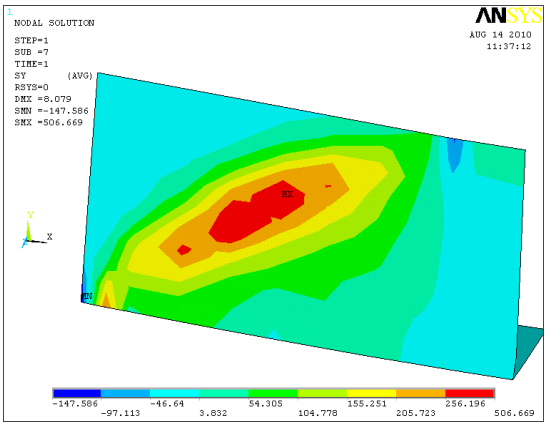

Figure 25 Variation of stresses of CFRP in y-direction along the analyzed quarter of RC beam (CP90U) at ultimate load.

6. Parametric Study

In order to investigate the effects of some material and solution parameters on the shear behavior of RC beams strengthened with FRP materials, the beams were analyzed in the previous paragraph, have been chosen carry out a parametric study.

6.1 Effect of Partial and Full Interaction between FRP Strips/sheets and Concrete Surface

In order to study the effect of full and partial interaction of the FRP strips/sheets mounted on the concrete surface of RC beams (CP90II), (CP90U), (GP90II) and (GP90U), the beams were analyzed assuming full contact (generated from concrete nodes) and using interface elements with TAUMAX equals to 5.5 MPa.

Figures (26 to 29) reveals that the numerical load–deflection curves are almost similar up to a load level equals to 35% of the ultimate load, after which the behavior with full interaction shows a stiffer response as compared with partial interaction case. The ultimate loads for the full interaction case, the ultimate loads obtained using partial interaction and the predicted ultimate load values obtained from this study are listed in Table 3.

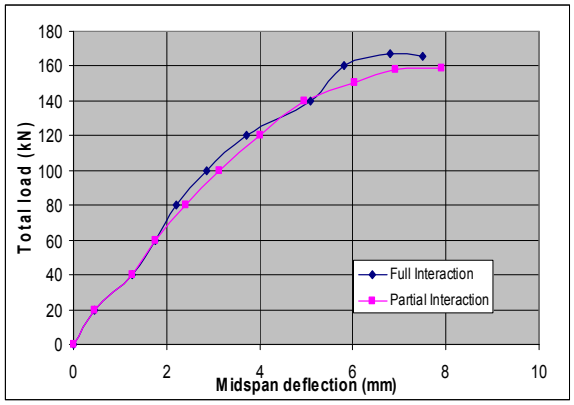

Figure 26 Effect of partial and full interaction on the behavior of RC beam (CP90II).

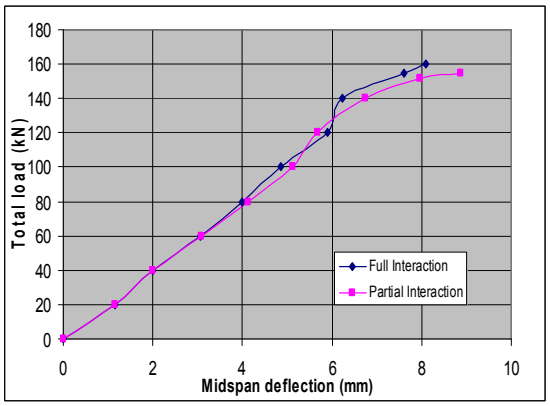

Figure 27 Effect of partial and full interaction on the behavior of RC beam (CP90U).

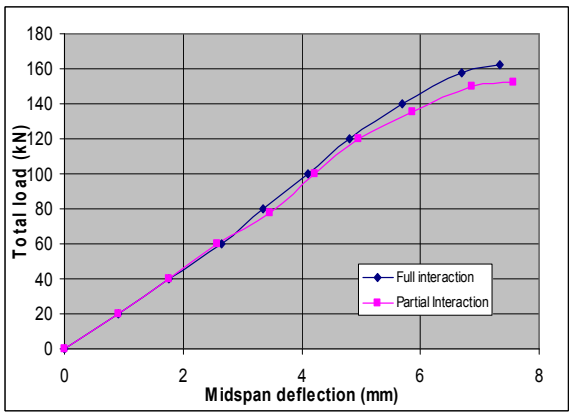

Figure 28 Effect of partial and full interaction on the behavior of RC beam (GP90II).

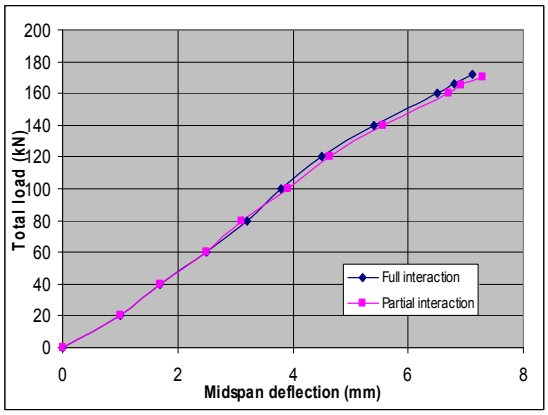

Figure 29 Effect of partial and full interaction on the behavior of RC beam (GP90U).

Table 3 Effect of partial and full interaction on the predicted ultimate loads of RC beams (CP90II), (CP90U), (GP90II) and (GP90U).

State of the beam	Numerical ultimate load with full interaction (kN)	Numerical ultimate load with partial interaction (kN)	$Pu_{full\ inter..}/Pu_{partial\ inter.}$
(CP90II)	166	159	1.044
(CP90U)	160	155	1.032
(GP90II)	162	152	1.065
(GP90U)	172	170	1.011

6.2 Distribution of FRP Materials Stresses

Figure 30 exhibits the load-stress relation for a typical vertical FRP strip of beams (CP90S), (GP90S) and (CS90), the figure shows that the stress of CFS slightly greater than CFRP strips stresses at the same load level, while the stresses in CFS and CFRP strips highly greater than GFRP strips stresses at the same load level. Figure 31 exhibits the load-stress relation for a typical vertical FRP sheet of beams (CP90S), (GP90S) and (CS90), the figure shows that the stress of CFS sheets slightly greater than CFRP sheets stresses at the same load level, while the stresses in CFS and CFRP sheets highly greater than GFRP sheets stresses at the same load level.

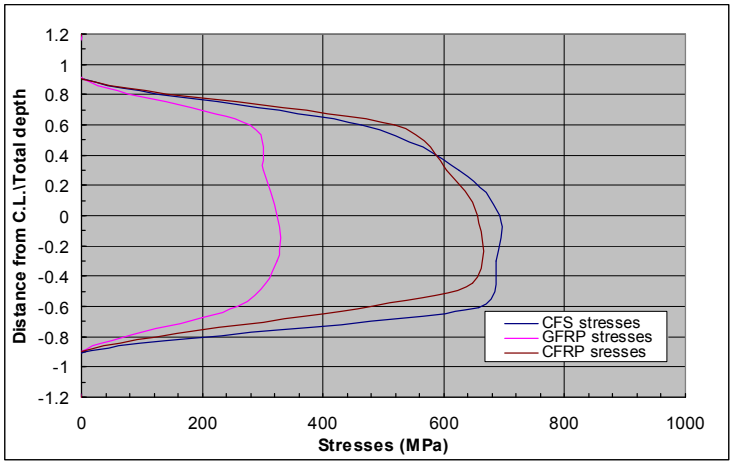

Figure 30 stresses in a typical vertical FRP strips at load level (P=160 kN).

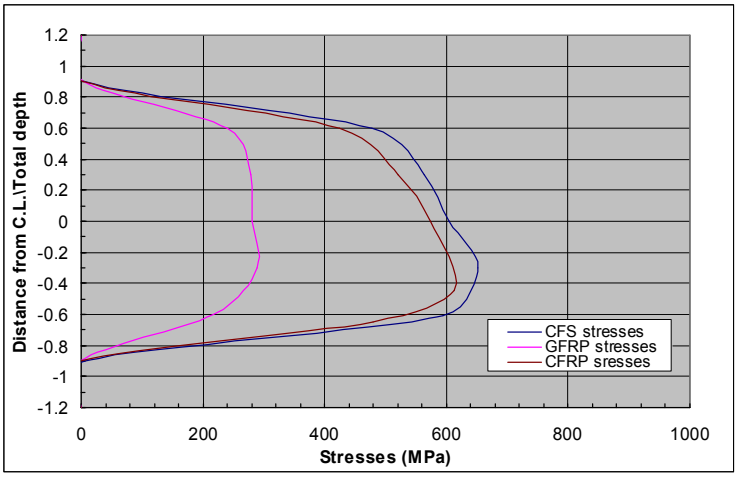

Figure 31 stresses in a typical vertical FRP sheets at load level (P=125 kN).

The ultimate stresses values of FRP materials at load level (P=160 kN) for strips and load level (P=125 kN) for sheets obtained from this study are listed in Table 4.

Table 4 Ultimate stresses value of FRP materials of RC beams (CP90II), (CP90U), (GP90II), (GP90U), (CS90II) and (CS90S).

State of the beam	*Load level (kN)*	*Stresses (Mpa)*
(CP90S)	160	655
(CP90II)	125	617
(GP90S)	160	323
(GP90II)	125	280
(CS90II)	160	692
(CS90S)	125	652

6.3 Crack Patterns

In ANSYS computer program the fractured cracking or crushing types of fracture occurred at concrete elements are indicated as circles located at sampling points. The designations of crack and crush types of fracture are summarized as follows:

1. Cracking is shown with a circle outline in the plane of the crack.
2. Crushing is shown with an octahedron outline.
3. If a certain crack has opened and then closed, the circle outline will have an X mark through the corresponding circle.

Each integration point of a brick element can crack in up to three different planes. The first crack occurred at an integration point is shown with a red circle outline, the second crack is presented with a green circle outline, and the third crack is shown with a blue circle outline [3]. In the present study, RC control beam (CON), RC beam (CP90S) and RC beam (CP90II) were selected as examples to present the crack pattern and crushing regions at different levels of loading.

Figures (32 to 34) show the crack patterns in front face of quarter RC control beam (CON), RC beam (CP90S) and RC beam (CP90II), respectively, at different stages of loading. Figure 32 reveals that flexure cracks occur at mid-span region with diagonal shear cracks being to propagate at a load level of 50 kN.

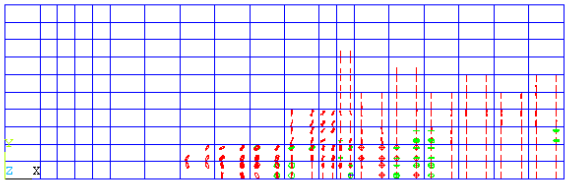

a. Crack pattern for RC beam (CON) at load level of 50 kN (0.52 P_u).

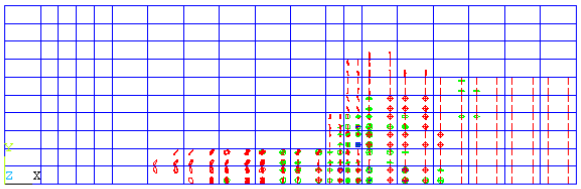

b. Crack pattern for RC beam (CON) at load level of 70 kN (0.72 P_u).

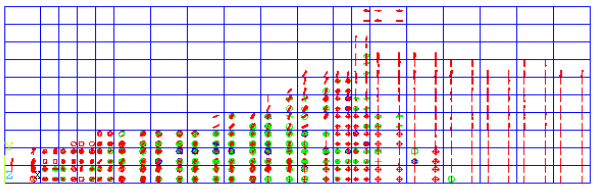

c. Crack pattern for RC beam (CON) at load level of 96 kN (P_u).

Figure 32 Crack pattern for RC control beam (CON) at different load level.

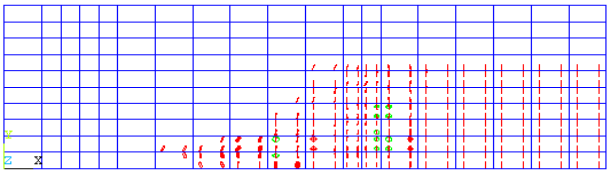

a. Crack pattern for RC beam (CP90S) at load level of 80 kN

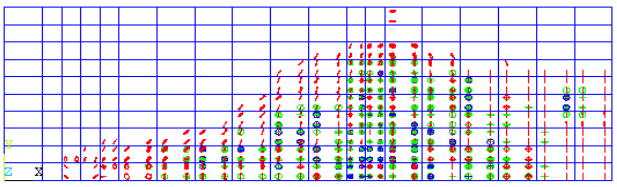

b. Crack pattern for RC beam (CP90S) at load level of 120 kN (0.75 P_u).

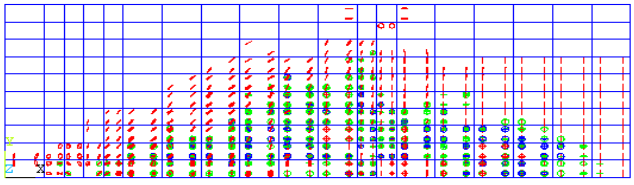

c. Crack pattern for RC beam (CP90S) at load level of 166 kN (P_u).

Figure 33 Crack pattern for RC beam (CP90S) at different load level.

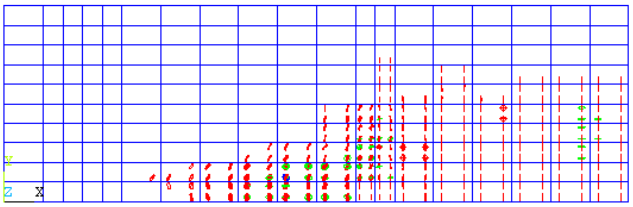

a. Crack pattern for RC beam (CP90II) at load level of 80 kN (0.5 P_u).

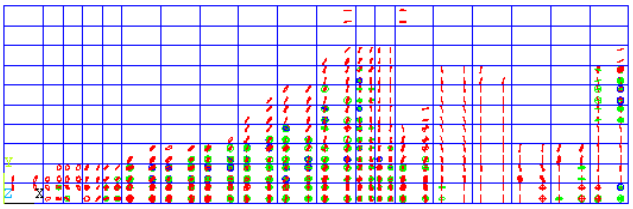

b. Crack pattern for RC beam (CP90II) at load level of 120 kN (0.75 P_u).

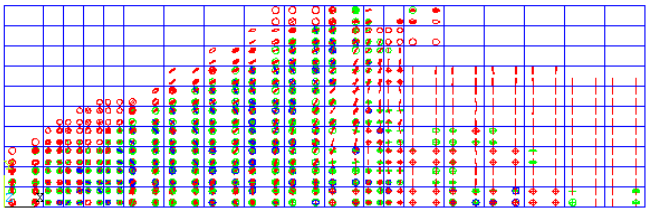

c. Crack pattern for RC beam (CP90II) at load level of 160 kN (P_u).

Figure 34 Crack pattern for RC beam (CP90II) at different load level.

Figures (32 to 34) show that, the cracks in RC beam strengthened with CFRP sheets more than the cracks in RC beam strengthened with CFRP strips and the cracks in RC beam strengthened with CFRP strips more than the cracks in RC control beam at the same level of loading.

7. Conclusions

The conclusions drawn for RC beams strengthening by FRP materials based on the finite element analyses carried out in this study are presented as:

1. In general, the results obtained using the finite element models represented by the load midspan deflection curves show good agreement with the experimental data for the beams considered in this study.
2. For the beams (CP90II), (CP90U), (GP90II) and (GP90U), which have been analyzed by assuming partial interaction between the CFRP strips and concrete surface using interface elements, the ultimate load is decreased by about 4.2%, 3.12%, 6.17% and 1.16%, respectively, as compared with full interaction case.
3. The ultimate loads in RC beams strengthened with CFRP strips and CFS greater than the ultimate loads in RC beams strengthened with CFRP and CFS sheets, while the ultimate load in RC beam strengthened with GFRP strips lower than the ultimate load in RC beam strengthened with GFRP sheets, this is because the tensile strength of CFRP and CFS don't reach the ultimate while in GFRP may be reach to ultimate due to closed to yield stress of steel reinforcement.
4. The RC beams strengthened with FRP sheets sustained cracks more than the RC beam strengthened with FRP strips and the RC beam strengthened with FRP strips sustained cracks more than the RC beam without strengthened.

8. References

1. Klaiber, F.W.; Wipf, J.J and Kempers .B.J., **"Repair *of Damaged Prestressed Concrete Bridges using CFRP*"**, proceedings of the 2003 Mid. Transportation Research Symposium, Ames, lowa, August 2003. © 2003 by lowa state University, www.ctre.iastate.edu.

2. American Concrete Institute, **"*Guide for the Design and Construction of Externally Bonded FRP Systems for Strengthening Concrete Structures*"** ACI-440.2R-02, Farmington Hill, Michigan, (2002), pp. 1-45.

3. ANSYS, "*ANSYS Help*", Release 12.0, Copyright 2009.

4. Dawe, D. J., "***Matrix and Finite Element Displacement Analysis of Structures***", Clarendon Press, Oxford, U. K., 1984, 565 pp.

5. Turner, M. C., Martin, R. H., and Topp, L., "***Stiffness and Deflection Analysis of Complex Structures***", Journal of Aeronautical Sciences, Vol. 23, No. 9, September, 1956, pp. 805-823.

6. Phillips, D. V., and Zienkiewics, O. C., "***Finite Element Nonlinear Analysis of Concrete Structures***", Journal of Structural Division, ASCE Proceedings, Part 2, Vol. 61, 1976, pp. 59-88.

7. Chen, W. F., and Saleeb, A. F., "***Constitutive Equations for Engineering Materials***", West Lafayette, Indiana, 1981, 580 pp.

8. William, K. J. and Warnke, E. p., "***Constitutive Model for the Triaxial Behavior of Concrete***", Proceedings, International Association for Bridge and Structural Engineering, Vol. 19, ISMES, Bergamo, Italy, 1975, 174 pp.

9. Saadatmanesh, H. and Malek, A.M., "***Design Guidelines for Flexural Strengthening of RC Beams with FRP Plates***", Journal of Composite for Construction, Vol.2, No.4, November, 1998, pp. 158-164.

10. Sim J., Kim G., Park C., and Ju M., "Shear Strengthening Effects with Varying Types of FRP Materials and Strengthening Methods" pp. 1665-1678.

11. ACI Committee 440 (2002), **"*Guide for the Design and Construction of Externally Bonded FRP Systems for Strengthening of Concrete Structures*"**, American Concrete Institute, Michigan, USA, 2002, 45 pp.

12. ACI Committee 318, "***Building Code Requirements for Structural Concrete (ACI 318M-08) and Commentary (ACI 318R-08)***", American Concrete Institute, Farmington Hills, MI, 2008, 466 pp.